RESEARCH ARTICLE | JULY 01 2022

Indirect physical mechanism of viscous forces: Vortex stretching and twisting

L. M. Lin (林黎明) ✉ ; Y. X. Wu (吴应湘)

Physics of Fluids 34, 073101 (2022)
https://doi.org/10.1063/5.0095838

Physics of Fluids ARTICLE scitation.org/journal/phf

Indirect physical mechanism of viscous forces: Vortex stretching and twisting

Cite as: Phys. Fluids **34**, 073101 (2022); doi: 10.1063/5.0095838
Submitted: 13 April 2022 · Accepted: 10 June 2022 ·
Published Online: 1 July 2022

View Online Export Citation CrossMark

L. M. Lin (林黎明),[1,a)] and Y. X. Wu (吴应湘)[1,2]

AFFILIATIONS

[1]Key Laboratory for Mechanics in Fluid Solid Coupling Systems, Institute of Mechanics, Chinese Academy of Sciences, Beijing 100190, China
[2]School of Engineering Sciences, University of Chinese Academy of Sciences, Beijing 100049, China

[a)]Author to whom correspondence should be addressed: llmbirthday@163.com

ABSTRACT

In this paper, the indirect physical mechanism of viscous forces, i.e., vortex stretching and twisting, is theoretically explored. The local flow in the immediate neighborhood of a flat plate is analyzed. Only the viscous forces are considered. By introducing oppositely signed streamwise vorticity in such a region, the induced velocity and vorticity fields are obtained. Because the induced streamwise velocity varies along with both the wall-normal and spanwise directions, induced vertical and spanwise vorticities are generated. The induction sequence is first clarified. Then, two indirect effects of viscous forces are identified. The induced spanwise vorticity leads to the original two-dimensional spanwise vorticity increasing and decreasing alternately across the span, as the vortex stretching effect of viscous forces. The local spanwise vortex is distorted at positions where the streamwise vorticity is introduced, and the appearance of induced vertical vorticity at the same positions enhances this effect, as the vortex twisting effect of viscous forces.

I. INTRODUCTION

It is already known that viscous and inertial forces play different physical roles in fluid mechanics and vortex dynamics.[1] The viscous forces due to large velocity gradients, such as boundary layers at solid surfaces, cause the generation of vorticity at walls and the diffusion of such vorticity. Once the vortex core is far away from the wall, such as the alternately shedding Kármán vortices, the vorticity diffusion further leads to the dissipation of vorticity in the center of the vortex. However, inertial forces have two physical mechanisms. One is the convective transport of vorticity with the local fluid velocity, typically illustrated by Kelvin's theorem. Another is the stretching of vortex lines, which intensifies the vorticity.

First, let us briefly review these different physical mechanisms of viscous and inertial forces. The fluid is incompressible with constant density ρ and kinematic viscosity ν. All body forces, such as gravity, are potential and, thus, can be simplified as a part of pressure. Then, the nondimensional momentum equation in an inertial frame of reference, such as the Cartesian coordinate system (x, y, z), can be written as

$$\frac{\partial \boldsymbol{u}}{\partial t} + (\boldsymbol{u}\cdot\nabla)\boldsymbol{u} = \frac{\mathrm{D}\boldsymbol{u}}{\mathrm{D}t} = -\nabla p + \frac{1}{Re}\nabla^2\boldsymbol{u}, \tag{1}$$

where $\boldsymbol{u} = (u, v, w)$ is the velocity vector with three components along with its own coordinates, t is the time, ∇ is the gradient operator, $\mathrm{D}/\mathrm{D}t$ is the Lagrangian derivative, p is the static pressure, and Re is the Reynolds number defined as $U_\infty L/\nu$, where U_∞ is the characteristic velocity and L is the characteristic length, such as the length of a flat plate or the base height of a bluff body. Velocities are scaled by U_∞ and lengths by L.

Then, the definition of the vorticity, $\boldsymbol{\omega}$, of a flow field, i.e., the curl of the velocity $\boldsymbol{u}$, gives $\boldsymbol{\omega} = \nabla\times\boldsymbol{u}$. Taking the curl of the momentum equation, Eq. (1) gives

$$\frac{\partial \boldsymbol{\omega}}{\partial t} + (\boldsymbol{u}\cdot\nabla)\boldsymbol{\omega} = \frac{\mathrm{D}\boldsymbol{\omega}}{\mathrm{D}t} = (\boldsymbol{\omega}\cdot\nabla)\boldsymbol{u} + \frac{1}{Re}\nabla^2\boldsymbol{\omega}. \tag{2}$$

In this equation, the last term on the right side, $\nabla^2\boldsymbol{\omega}/Re$, is simply the vorticity diffusion. The term, $(\boldsymbol{u}\cdot\nabla)\boldsymbol{\omega}$ represents the convective transport of vorticity, as the first effect of inertial forces. The term, $(\boldsymbol{\omega}\cdot\nabla)\boldsymbol{u}$ represents vortex stretching in a segment of fluid with vorticity, as the second effect of inertial forces. Furthermore, as shown in Fig. 1, this nonlinear term, $(\boldsymbol{\omega}\cdot\nabla)\boldsymbol{u}$, can be rewritten as follows:

$$(\boldsymbol{\omega}\cdot\nabla)\boldsymbol{u} = |\boldsymbol{\omega}| \lim_{\mathrm{P_2P_1}\to 0} \frac{\delta \boldsymbol{u}}{\mathrm{P_2P_1}} = |\boldsymbol{\omega}| \lim_{\delta l\to 0} \frac{\delta \boldsymbol{u}}{\delta l}, \tag{3}$$

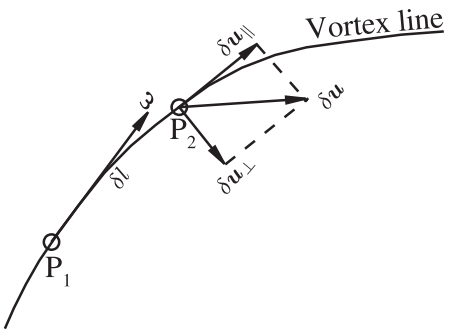

FIG. 1. Schematic diagram of vortex stretching and twisting in the nonlinear term $(\boldsymbol{\omega} \cdot \nabla)\boldsymbol{u}$.

where P_1 and P_2 are two adjacent points on the vortex line with a distance of δl, and $\delta \boldsymbol{u}$ is the relative velocity at point P_2 relative to the velocity at point P_1. Then, the local relative velocity vector $\delta \boldsymbol{u}$ can be divided into a component $\delta \boldsymbol{u}_{\parallel}$ parallel to the vortex line and a component $\delta \boldsymbol{u}_{\perp}$ perpendicular to the vortex line. Therefore, the vortex line can be stretched or compressed by component $|\boldsymbol{\omega}| \lim_{\delta l \to 0} \frac{\delta \boldsymbol{u}_{\parallel}}{\delta l}$ and twisted by component $|\boldsymbol{\omega}| \lim_{\delta l \to 0} \frac{\delta \boldsymbol{u}_{\perp}}{\delta l}$.

As a result of these vortex stretching and twisting mechanisms owing to the inertial forces, a kind of interaction between two vortices with perpendicular rotational directions is identified and analyzed in the wakes of different bluff bodies under the effects of geometric disturbances.[2,3] For example, in the wake of a flat plate at zero incidence with the introduction of periodic spanwise perturbations at a low Reynolds number of approximately 100, the streamwise interaction between the streamwise vortex pair (along the streamwise direction, i.e., the x-axis) and spanwise vortex (along the spanwise direction, i.e., the z-axis) is investigated experimentally and numerically,[2] as shown in Fig. 2(a). As the streamwise vortex tubes evolve, they interact with the spanwise vortices by lifting them up and pushing them down (in the vertical direction, i.e., the y-axis) in an alternating fashion across

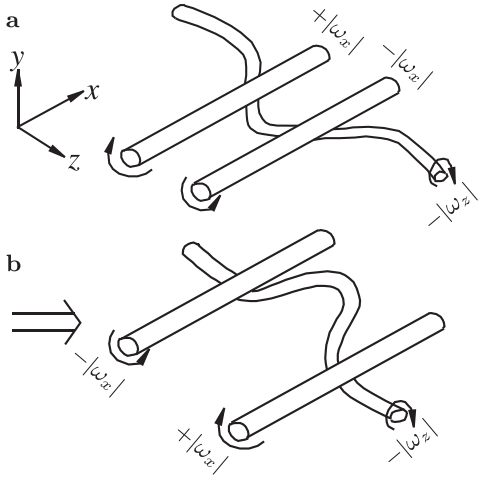

FIG. 2. Schematic diagrams of (a) the streamwise interaction between the streamwise vortex pair and spanwise vortex[2] and (b) the same streamwise interaction obtained by shifting the phase by half a wavelength.

the span. The resulting curvature of the spanwise vortices, in turn, causes further stretching and intensification of the streamwise vorticity. Thus, the interaction between the streamwise and spanwise vortices proceeds in a self-amplifying manner, resulting in the formation of closed vortex loops of alternating signs.[2] A similar mechanism has been reported in the wake of a square-section cylinder with wavy stagnation surfaces at a Reynolds number of 100.[4] The streamwise vortex pair induces a vertical velocity with a specific distribution within the top and bottom shear layers. As a result, an upwash and downwash (also on the y-axis) appear in a sinusoidal fashion. This undulation leads to both upper and lower shear layers wavily varying across the span as well as the wake width. Moreover, by shifting the phase by half a wavelength of oppositely signed streamwise vorticity, as shown in Fig. 2(b), the same streamwise interaction is obtained with the formation similar to the hairpin vortex appearing in the boundary layer, as introduced in the following context.

Generally, in flow past a flat plate at zero incidence, the experimental results demonstrating the appearance of hairpin vortices are shown in the basic sketch in Fig. 3(a). The transition in the laminar boundary layer is initially governed by stable laminar flow, the instability of traveling, two-dimensional (2D) Tollmien–Schlichting (T–S) waves, primary stability theory, and the appearance of unsteady, laminar, and three-dimensional (3D) waves due to secondary instabilities and a characteristic Λ-structure vortex formation,[5] as shown in Fig. 3(a). The 3D disturbance with increasing T–S instability waves leads to the formation of streamwise vortex pairs in the neighborhood of the

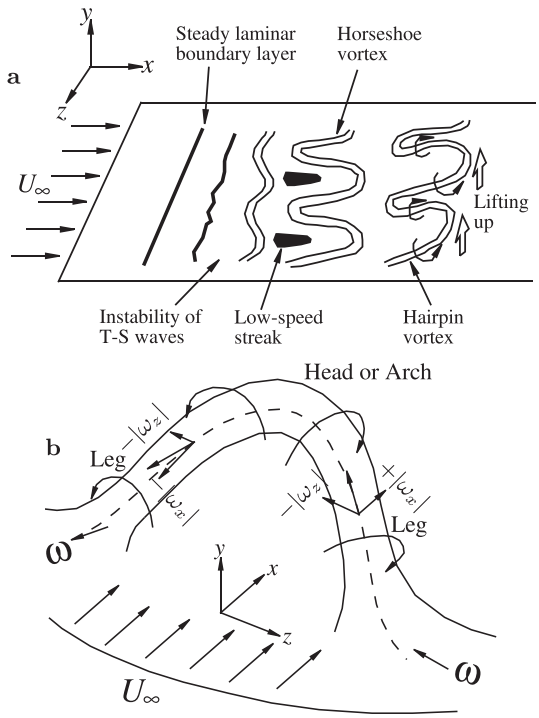

FIG. 3. Schematic diagrams of (a) the formation of Tollmien–Schlichting waves and horseshoe and hairpin vortices in the transition of the laminar boundary layer of a flat plate at zero incidence, and (b) Theodorsen's conceptualized picture of a hairpin vortex with the vorticity decomposition at two legs.[11]

laminar boundary layer.[6] This periodic distribution of streamwise vortex pairs along the span further results in the redistribution of the streamwise velocity along the span, forming staggered streaks with high and low speeds in the buffer region.[7] The streaks and the vortices are involved in a self-sustaining nonlinear cycle.[8,9] Meanwhile, the signal of velocity fluctuations is characterized by so-called spikes which denote the appearance of local high shearing regions together with the point of inflection velocity profiles. With increasing disturbance, streamwise vortex pairs around low-speed streaks develop into a horseshoe vortex.[10] The horseshoe vortex is lifted up under self-induction and elongated due to the external shear flow and thus becomes a hairpin vortex. Although there is no unique and generally accepted quantitative definition of a hairpin, it is described as a category of vortices consisting of a head (or a negatively rotating arch, thus with the negative spanwise vorticity) oriented in the spanwise direction and two adjacent legs extending upstream and wall-ward.[6] The classic hairpin (or horseshoe) vortex paradigm was originally proposed by Theodorsen,[11] as shown in Fig. 3(b). Such a hairpin vortex can also be generated by introducing the sinuous perturbation of the spanwise velocity[12] and an isolated cuboid roughness and a short duration jet in the boundary layer.[13]

Furthermore, by comparing the streamwise interaction in Fig. 2(b) and the hairpin vortex in Fig. 3(b) with an analysis of vorticity components at two legs, the similarity in the twisted spanwise vortex and the local periodical distribution of oppositely signed streamwise vorticity indicates a certain kind of intrinsic physical relationship. Recently, through a theoretical analysis of Theodorsen's hairpin vortex in the immediate neighborhood of a flat plate in a laminar boundary layer, the lifting-up mechanism was mainly attributed to the vortex-induced vortex (VIVor) mechanism, as a result of viscous forces.[14] Since only the viscous forces are considered in this analysis, there is speculation that the spanwise vortex stretching and twisting in both cases, i.e., the streamwise interaction and the hairpin vortex, can also be realized by the viscous forces, regardless of the degree of this stretching or twisting.

To the best of our knowledge, there is no literature addressing this potential physical mechanism of viscous forces. Therefore, the main aim of this study is to further explore this subject through theoretical analysis of a local flow in the immediate neighborhood of solid walls, as the basic flow with the dominant viscous forces. The central issue is the condition for this vortex stretching and twisting mechanism due to viscous forces.

II. ANALYTICAL MODEL

As shown in Fig. 4, the 2D flow is over a flat plate at zero incidence. First, the Cartesian coordinate system (x, y, z) is established as follows: the x-axis is aligned with the flow direction, referred to as the streamwise direction; the y-axis is the wall-normal direction, referred to as the vertical direction; and the z-axis is referred to as the spanwise direction across the span. In such flow, the incoming velocity U_∞ is uniform across the span and assumed to vary only along the wall-normal direction.

Since only viscous forces are balanced with the (friction) pressure gradient, the dimensionless mass continuity equation and the momentum equation are written by

$$\nabla \cdot \boldsymbol{u} = 0, \tag{4a}$$

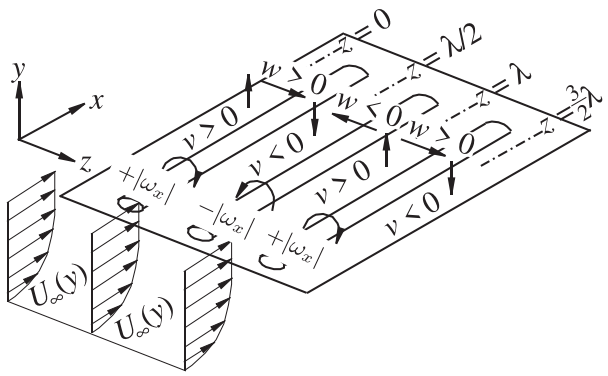

FIG. 4. Schematic diagram of oppositely signed streamwise vortex pair, $\pm|\omega_x|$, periodically distributed on the flat plate and induced velocity field (v, w).

$$\nabla p = \frac{1}{Re}\nabla^2 \boldsymbol{u}. \tag{4b}$$

The vorticity transportation equation, Eq. (2), is simplified as

$$\nabla^2 \boldsymbol{\omega} = 0. \tag{5}$$

For the boundary condition, the nonslip boundary condition with velocity $\boldsymbol{u} = 0$ is applied at the solid surface of a flat plate $y = 0$.

Moreover, it is necessary to introduce the streamwise vortex pair with oppositely signed vorticity, as shown in Fig. 4. These streamwise vortices at solid walls may be generated due to geometric disturbances, such as wavy stagnation surfaces on the square-section cylinder, artificial disturbances, such as wall blowing or suction, or natural disturbance velocity caused by the three-dimensional instability or turbulence. For the sake of convenience, these introduced streamwise vortices are assumed to be uniform along the streamwise direction and periodical along the spanwise direction. The streamwise length scale and spanwise wavelength λ are finite and mainly determined according to the above vorticity generation mechanism.

Based on the above analysis, the flow analysis closely correlates with Reynolds number Re. In the laminar flow, such disturbed streamwise vorticity is mainly caused by introducing (e.g., geometric) disturbances. Reynolds number is then defined by the characteristic length L of a bluff body. Since the introduced spanwise wavelength λ is on the order of such length L, the Reynolds number can also be defined by λ. However, in the turbulent flow, this disturbed streamwise vorticity can result from the small-scale eddy motion. Therefore, λ is much smaller than L. The local Reynolds number Re_λ in the present flow region can be defined by λ, i.e., $Re_\lambda = U_\infty \lambda/\nu$, also considerably smaller than the Reynolds number defined by L. Thus, Re_λ can be used in the present disturbed flow, regardless of laminar or turbulent flow.

Whether in laminar or turbulent flow, the analyzed flow region is the immediate neighborhood of solid walls. The streamwise size L_x in this region is finite until the boundary condition of vorticity at walls qualitatively changes.[14,15] The vertical size L_y is also finite until viscous forces are no longer dominant. For example, in the turbulent boundary layer, L_y is less than five viscous lengths. This flow region is the viscous sublayer.

Because of the linear feature in Eqs. (4a) and (5), the local velocity and vorticity fields can be decomposed into two parts:

(1) Original 2D shear flow: the 2D velocity field with $U(y) = U_\infty(y)$ and $V = W = 0$, and only 2D spanwise vorticity with $\Omega_z(y) = -\frac{\partial U}{\partial y}$, similar to the spanwise vortex tube generated on solid walls due to the fluid viscosity;
(2) 3D induced flow field: the 3D induced velocity (u, v, w) and vorticity $(\omega_x, \omega_y, \delta\omega_z)$ in which the induced spanwise vorticity $\delta\omega_z = \omega_z - \Omega_z$.

We mainly focus on the latter and investigate the effect of the latter on the former. Here, the local flow region $(0 < x < L_x, 0 < y < L_y)$ with $\Omega_z < 0$ is taken into account. The 3D induced flow field is also solved by Eqs. (4a) and (5).

III. RESULTS AND DISCUSSION

According to VIVor theory, the qualitative results for two or three kinds of boundary cases are exactly the same.[14,15] Here, only the first boundary case, in which the streamwise vorticity with the greatest intensity is generated on the wall and gradually decreases when the vertical distance is far from the wall, is adopted for simplicity in the following analysis. The induced streamwise velocity u is assumed to be zero at the origin of $x = 0$ in Fig. 4. In addition, only the results of the induced velocity and vorticity fields are presented here, and the deduction process is referenced in previous works.[14,15]

Moreover, to better illustrate the following qualitative analysis, the case, in which a flow passes a circular cylinder under harmonic disturbance with nondimensional wavelength $\lambda = 6$ and wave height $W = 0.6$ at $Re = 100$, is simulated with the full Navier–Stokes equation in Eq. (1),[16] as shown in Figs. 5 and 6.

According to the VIVor theory in the first boundary case, the exact solutions of the induced velocity field can be written by

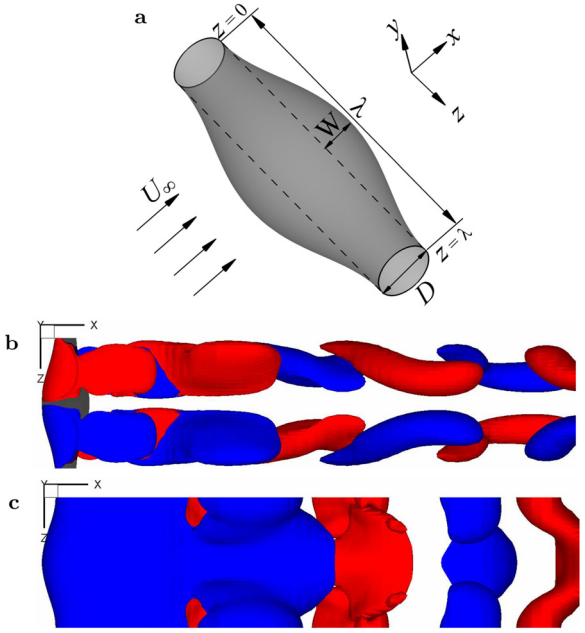

FIG. 5. (a) Schematic diagram of a uniform flow past a circular cylinder with the harmonic disturbance, and iso-surfaces of (b) $\omega_x = \pm 0.2$ and (c) $\omega_z = \pm 0.2$ at $t = 390$, $\lambda = 6$, $W/\lambda = 0.1$ and $Re = 100$, where red and blue colors denote positive and negative values, respectively.

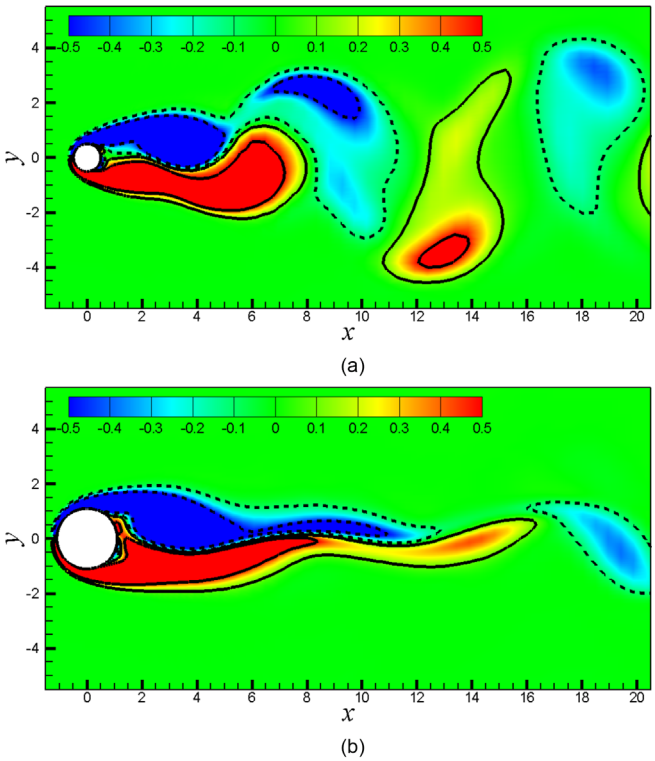

FIG. 6. Contours of ω_z at (a) $z = 0$ and (b) $z = \frac{1}{2}\lambda$ in the case of Fig. 5, where solid and dashed lines of $\omega_z = \pm 0.1$ and ± 0.5 denote positive and negative values, respectively.

$$u = -C_2 x(e^{\beta y} - e^{-\beta y})\cos(\beta z), \tag{6a}$$

$$v = \left[\left(\frac{C_2}{2}y - \frac{C_1}{4\beta}\right)(e^{\beta y} - e^{-\beta y}) + \frac{C_1}{2}ye^{-\beta y}\right]\cos(\beta z), \tag{6b}$$

$$w = \left[\frac{1}{2\beta}\left(\frac{C_1}{2} + C_2\right)(e^{\beta y} - e^{-\beta y}) + \frac{C_1}{2}ye^{-\beta y} - \frac{C_2}{2}y(e^{\beta y} + e^{-\beta y})\right]\sin(\beta z), \tag{6c}$$

where $\beta = 2\pi/\lambda$ is the wavenumber, and C_1 and C_2 are positive constants with the basic relationship of $C_2 \geq 2C_1$. The exact solutions for the vorticity field are also given by

$$\omega_x = \frac{\partial w}{\partial y} - \frac{\partial v}{\partial z} = C_1 e^{-\beta y}\sin(\beta z), \tag{7a}$$

$$\omega_y = \frac{\partial u}{\partial z} - \frac{\partial w}{\partial x} = \frac{\partial u}{\partial z} = C_2\beta x(e^{\beta y} - e^{-\beta y})\sin(\beta z), \tag{7b}$$

$$\delta\omega_z = \frac{\partial v}{\partial x} - \frac{\partial u}{\partial y} = -\frac{\partial u}{\partial y} = C_2\beta x(e^{\beta y} + e^{-\beta y})\cos(\beta z), \tag{7c}$$

$$\omega_z = \frac{\partial v}{\partial x} - \frac{\partial(U+u)}{\partial y} = -\frac{\partial U}{\partial y} - \frac{\partial u}{\partial y} = \Omega_z(y) + C_2\beta x(e^{\beta y} + e^{-\beta y})\cos(\beta z). \tag{7d}$$

Based on this induced flow field, as indicated in Eqs. (6) and (7), some results can be obtained and discussed as follows:

- Generation of vertical vorticity: because the vertical vorticity ω_y is aligned with the wall-normal direction, it is always zero at solid surfaces ($y = 0$); therefore, when the vertical position is away from the surface, nonzero vertical vorticity indicates that it is actually generated by introducing streamwise vortices, referred to as the VIVor mechanism, as reported in previous works.[14,15]
- Vorticity sign law: there is a special sign relationship between induced streamwise and vertical vorticities, $\omega_x\omega_y \geq 0$, in the present flow region ($x > 0, y > 0$), as already reported in previous works;[14,15] this indicates that where ω_x is greater or less than zero, ω_y is also greater or less than zero.
- Variation in the induced spanwise vorticity: as indicated in Eqs. (7d) and (7c), the induced spanwise vorticity, $\delta\omega_z$, is greater than zero at $z = 0$ and λ, but less than zero at $z = \frac{1}{2}\lambda$ and $\frac{3}{2}\lambda$.
- Variation of (total) spanwise vorticity: as indicated in Eq. (7d), corresponding to the sinusoidal variation of induced spanwise vorticity, (total) spanwise vorticity also varies across the span; for example, at $z = 0$ or λ, $\omega_z = \Omega_z(y) + C_2\beta x(e^{\beta y} + e^{-\beta y})$ and $|\omega_z| < |\Omega_z|$ due to $\delta\omega_z > 0$, denoting $|\omega_z|$ decreasing, while at $z = \frac{1}{2}\lambda$, $\omega_z = \Omega_z(y) - C_2\beta x(e^{\beta y} + e^{-\beta y})$ and $|\omega_z| > |\Omega_z|$ owing to $\delta\omega_z < 0$, denoting $|\omega_z|$ increasing.
- Spanwise-averaged induced and total spanwise vorticities: the spanwise-averaged vorticity is first defined as $\bar{\omega} = \frac{1}{\lambda}\int_0^\lambda \omega dz$; then, based on Eqs. (7c) and (7d), spanwise-averaged induced and total spanwise vorticities can be obtained as follows:

$$\begin{aligned}\overline{\delta\omega}_z &= \frac{1}{\lambda}\int_0^\lambda \delta\omega_z(x,y,z)\mathrm{d}z \\ &= \frac{1}{\lambda}\int_0^\lambda \left[C_2\beta x(e^{\beta y} + e^{-\beta y})\cos(\beta z)\right]\mathrm{d}z \\ &= 0, \end{aligned} \tag{8a}$$

$$\begin{aligned}\bar{\omega}_z &= \frac{1}{\lambda}\int_0^\lambda \omega_z(x,y,z)\mathrm{d}z \\ &= \frac{1}{\lambda}\int_0^\lambda \left[\Omega_z(y) + C_2\beta x(e^{\beta y} + e^{-\beta y})\cos(\beta z)\right]\mathrm{d}z \\ &= \Omega_z(y), \end{aligned} \tag{8b}$$

  which indicates that there is no variation in the spanwise-averaged flux of total spanwise vorticity within a wavelength λ because of $\overline{\delta\omega}_z = 0$; in other words, although disturbed streamwise vorticities with opposite signs are introduced periodically, the total flux of ω_z in one whole period is equivalent to the original 2D vortex flux.
- Induction process of induced velocity and vorticity: as indicated in Eq. (6), v and w are first induced by the introduced streamwise vorticity; then, owing to the continuity equation, Eq. (4a), u is generated and varies considerably across the span; consequently, the definition of vertical vorticity in Eq. (7b) indicates the induction of vertical vorticity wavily varying along the spanwise direction. Meanwhile, the vertical gradient of u also results in the appearance of $\delta\omega_z$ wavily varying across the span.
- Vortex stretching and compression: as for the original 2D spanwise vortex with vorticity Ω_z, the introduction of streamwise vortices induces the generation of induced spanwise vorticity $\delta\omega_z$ first, and then leads to (total) spanwise vorticity ω_z wavily varying across the span. Similar to the compressibility effect of a fluid on a vortex[1] or the stretching of inertial forces, the decrease in ω_z at $z = 0$ and λ correspond to vortex compression, while the increase in ω_z at $z = \frac{1}{2}\lambda$ corresponds to vortex stretching. As shown in Fig. 5 for a flow past a harmonic cylinder at $Re = 100$, the harmonic disturbance on a cylinder surface leads to the generation of oppositely signed streamwise vorticity in the near wake; the spanwise vorticity obviously varies across the span. Moreover, as shown in Fig. 6, the spanwise vorticity is diffused at $z = 0$ but concentrated at $z = \frac{1}{2}\lambda$; from the point of the isosurface or contour of ω_z, for example, the region of $\omega_z = \pm 0.1$ in Fig. 6 at $z = 0$ is larger than that at $z = \frac{1}{2}\lambda$. Accordingly, the previous sketch in Fig. 2 with uniform variation is inappropriate; taking into account the above spanwise variation of ω_z, it should be illustrated in Fig. 7; therefore, the vortex stretching due to viscous forces is clearly demonstrated by the wavily varied intensity of spanwise vortex in Fig. 7.

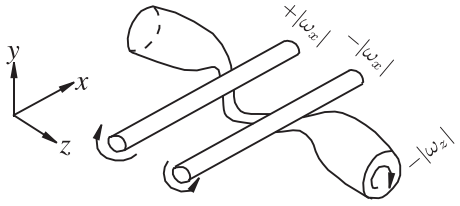

FIG. 7. Schematic diagram of wavily varied spanwise vortex with spanwise vorticity $-|\omega_z|$ owing to the effect of the introduced streamwise vortex pair with streamwise vorticity $\pm|\omega_x|$.

- Vortex twisting: corresponding to the sinusoidal variation in the intensity of the spanwise vortex in Fig. 7, the spanwise vortex tube is distorted mainly at positions where the streamwise vortex is introduced, such as $z = \frac{1}{4}\lambda$ and $\frac{3}{4}\lambda$, as shown in Fig. 5(c). On the contrary, as stated in "generation of vertical vorticity" and "vorticity sign law" above, the appearance of oppositely signed vertical vorticity further twists the original 2D spanwise vortex tube along the vertical direction at the same positions, where the streamwise vortex pair is introduced and the vertical velocity is just zero in Eqs. (6b) and (6c). Eq. (6b). Consequently, as analyzed in previous work,[14] the two legs of the hairpin vortex are lifted up, as is the hairpin vortex, as shown in Fig. 3(b). Finally, the original 2D vortex tube is totally twisted and becomes the hairpin vortex only under the effect of viscous forces.

IV. CONCLUSIONS

In this study, the potential physical mechanism of viscous forces, that is, vortex stretching and twisting, is theoretically analyzed and discussed. Because of the similarity between the streamwise interaction in the wake of a bluff body and the hairpin vortex in the boundary layer, the local flow in the immediate neighborhood of a flat plate, where the viscous forces are dominant and the inertial forces are neglected, is investigated.

In the analysis, there are two key conditions. As the first key condition, the nonslip boundary condition is applied on solid surfaces. As a result, a large velocity gradient can be generated due to the fluid viscosity, regardless of streamwise or spanwise vorticity, which is tangential to the wall. Another key condition is the induction or generation

of streamwise vorticity, caused by 3D geometric or artificial disturbances or disturbed velocity owing to the 3D instability or turbulence. This introduction of streamwise vorticity is a kind of initial disturbance in the original 2D shear flow.

Consequently, under these two key conditions and only viscous forces, the induced velocity and vorticity fields appear sequentially. First, v and w are induced by introduced streamwise vorticity. Then, u appears owing to the continuity equation. Because u varies across the span, vertical vorticity is generated, as one induced result of the introduced streamwise vortex. Meanwhile, since u also varies in the wall-normal direction, induced spanwise vorticity is generated, as another induced result of the introduced streamwise vortex. Finally, the total spanwise vorticity is changed along the spanwise direction.

Therefore, associated with this intensity variation of spanwise vorticity across the span, this effect of viscous forces is similar to the vortex stretching by intensifying the vorticity and the vortex compression by reducing the vorticity. However, as another effect of viscous forces, the original 2D spanwise vortex tube with wavily varied intensity is distorted at positions where the streamwise vortex is introduced, and the local vortex line is twisted because of the appearance of induced vertical vorticity. Considering that vortex stretching and twisting appear under the above two key conditions, the physical mechanism of viscous forces is indirect.

From the above statement, a more profound physical problem is proposed here: if viscous forces can also produce the effect of vortex stretching and twisting under certain conditions, then from the perspective of the physical mechanism of vortex stretching and twisting itself, what is its physical source or origin? Is it viscous force or inertial force? In other words, the viscous forces initially produce vortex stretching and twisting, and then the inertial forces reinforce such a physical effect; conversely, the inertial forces initially lead to vortex stretching and twisting, and the viscous forces thus intensify this physical mechanism. This will be further investigated in future work.

AUTHOR DECLARATIONS

Conflict of Interest

The authors have no conflicts to disclose.

DATA AVAILABILITY

The data that support the findings of this study are available from the corresponding author upon reasonable request.

REFERENCES

[1]S. I. Green, 1995 *Fluid Votices* (Kluwer Academic Publishers, Norwell).
[2]E. Meiburg and J. C. Lasheras, "Experimental and numerical investigation of the three-dimensional transition in plane wakes," J. Fluid Mech. **190**, 1–37 (1988).
[3]L. M. Lin, X. F. Zhong, and Y. X. Wu, "Effect of perforation on flow past a conic cylinder at Re = 100: Wavy vortex and sign laws," Acta Mech. Sin. **34**, 812–829 (2018).
[4]R. M. Darekar and S. J. Sherwin, "Flow past a square-section cylinder with a wavy stagnation face," J. Fluid Mech. **426**, 263–295 (2001).
[5]H. Schlichting, *Boundary Layer Theory*, 7th ed. (McGraw-Hall Book Company, 1979).
[6]M. R. Head and P. Bandyopadhyay, "New aspects of turbulent boundary layer structure," J. Fluid Mech. **107**, 297–338 (1981).
[7]S. J. Kline, W. D. Reynolds, F. A. Schraub, and P. W. Runstadler, "The structure of turbulent boundary layers," J. Fluid Mech. **30**, 741–773 (1967).
[8]J. Jiménez, G. Kawahara, M. P. Simens, M. Nagata, and M. Shiba, "Characterization of near-wall turbulence in terms of equilibrium and bursting solutions," Phys. Fluids **17**, 015105 (2005).
[9]W. Schoppa and F. Hussain, "Coherent structure generation in near-wall turbulence," J. Fluid Mech. **453**, 57–108 (2002).
[10]D. Swearingen and R. F. Blackwelder, "The growth and breakdown of streamwise vortices in the presence of a wall," J. Fluid Mech. **182**, 255–290 (1987).
[11]T. Theodorsen, "Mechanism of turbulence," in *Second Midwestern Conference on Fluid Mechanics* (Ohio State University, 1952), pp. 1–19.
[12]Y. S. Wang, W. X. Huang, and C. X. Xu, "On hairpin vortex generation from near-wall streamwise vortices," Acta Mech. Sin. **31**, 139–152 (2015).
[13]J. Yoshikawa, Y. Nishio, S. Izawa, and Y. Fukunishi, "Key structure in laminar-turbulent transition of boundary layer with streaky structures," Theor. Appl. Mech. Lett. **9**, 32–35 (2019).
[14]L. M. Lin and Y. X. Wu, "Theoretical analysis of vorticity in a hairpin vortex in the viscous sublayer of a laminar boundary layer," Eur. J. Mech. B Fluids **94**, 106–120 (2022).
[15]L. M. Lin, S. Y. Shi, X. F. Zhong, and Y. X. Wu, "Mechanism of wavy vortex and sign laws in flow past a bluff body: Vortex-induced vortex," Acta Mech. Sin. **35**, 1–14 (2019).
[16]L. M. Lin, X. F. Zhong, and Y. X. Wu, "Flow around a circular cylinder with radial disturbances at a low Reynolds number," in *Proceedings of the Twenty-Third International Offshore and Polar Engineering* (Anchorage, AL, 2013), pp. 387–394.